Electronic Supplementary Material (ESI) for Physical Chemistry Chemical Physics.

[Supplementary Information]

Probing the Microscopic Structural Organization of Neat Ionic Liquids (ILs) and Ionic Liquid- Based Gel through Resonance Energy Transfer (RET) Studies

Debashis Majhi and Moloy Sarkar*

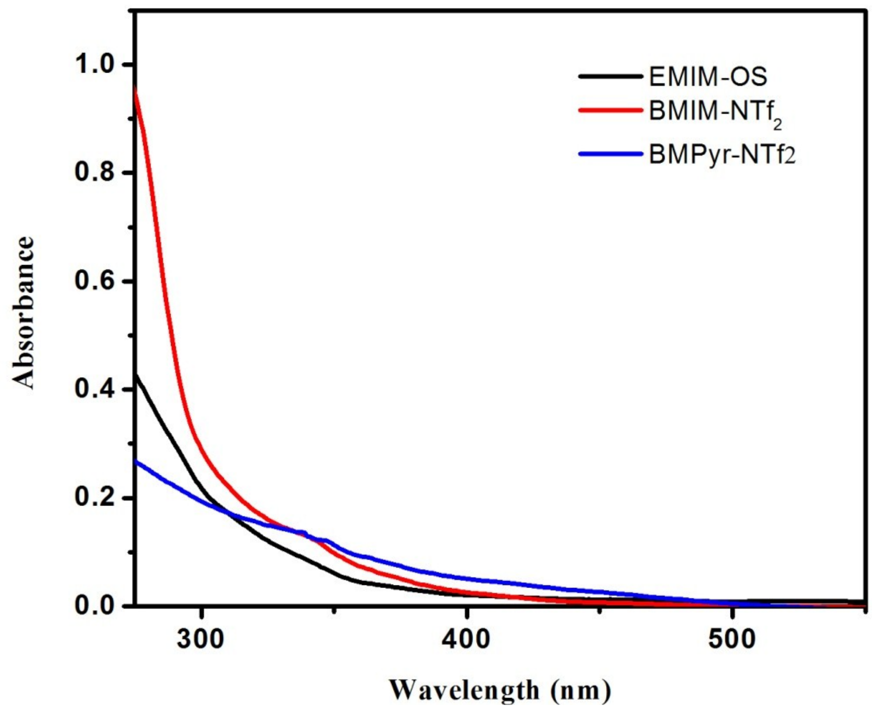

Fig. S1 Absorption spectra of EMIM-OS, BMIM-NTf$_2$ and BMPyr-NTf$_2$.

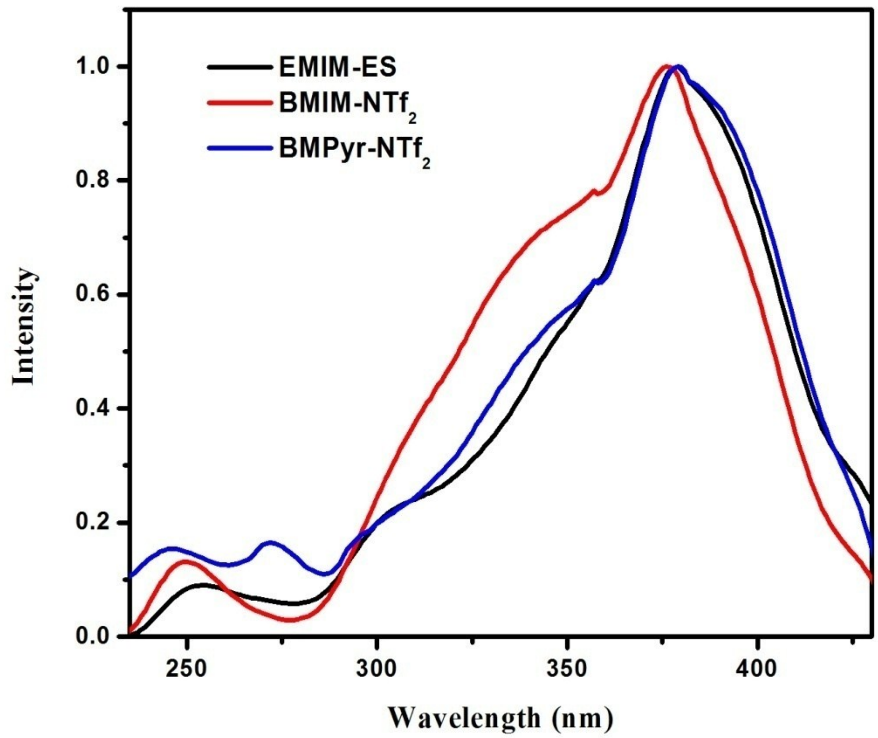

Fig. S2 Normalized excitation spectra of EMIM-ES, BMIM-NTf$_2$ and BMPyr-NTf$_2$.

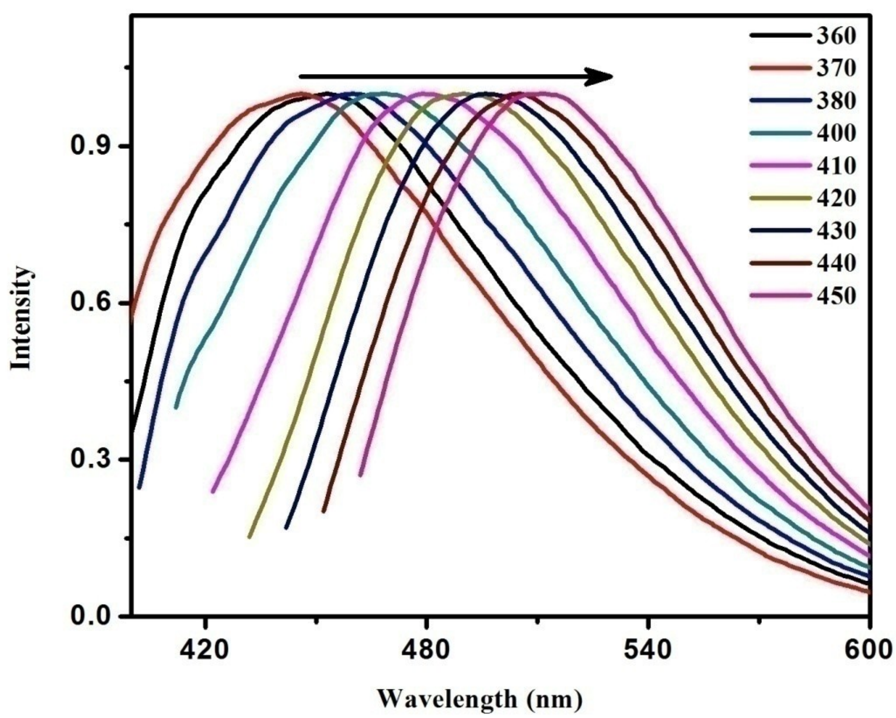

Fig. S3 Normalized emission spectra of EMIM-ES at different excited wavelength (λ_{exc}= 360-450 nm).

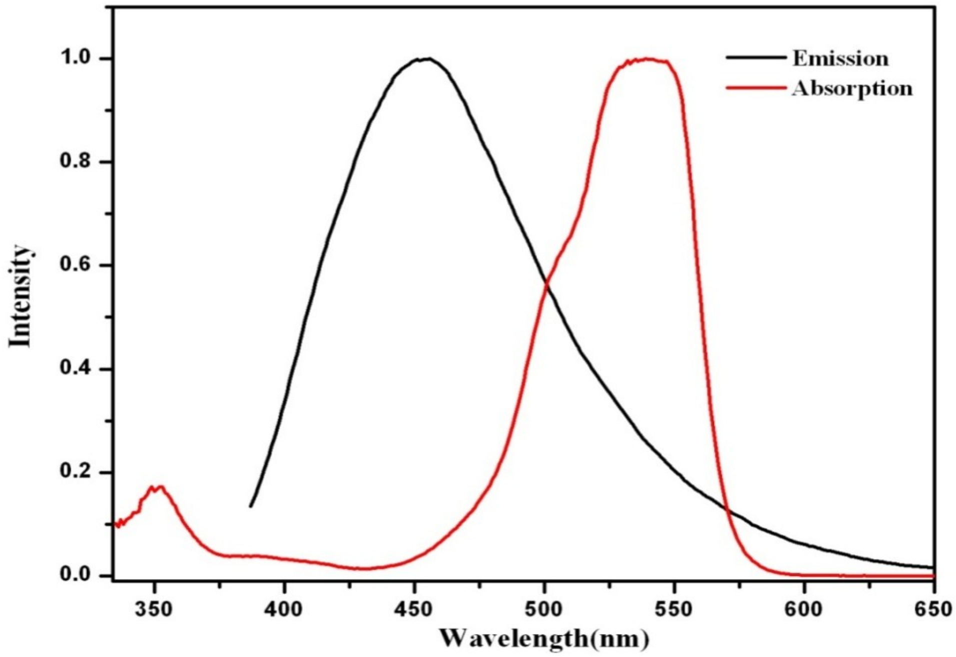

Fig. S4 Normalized absorption and emission spectrum of R6G and EMIM-OS respectively.

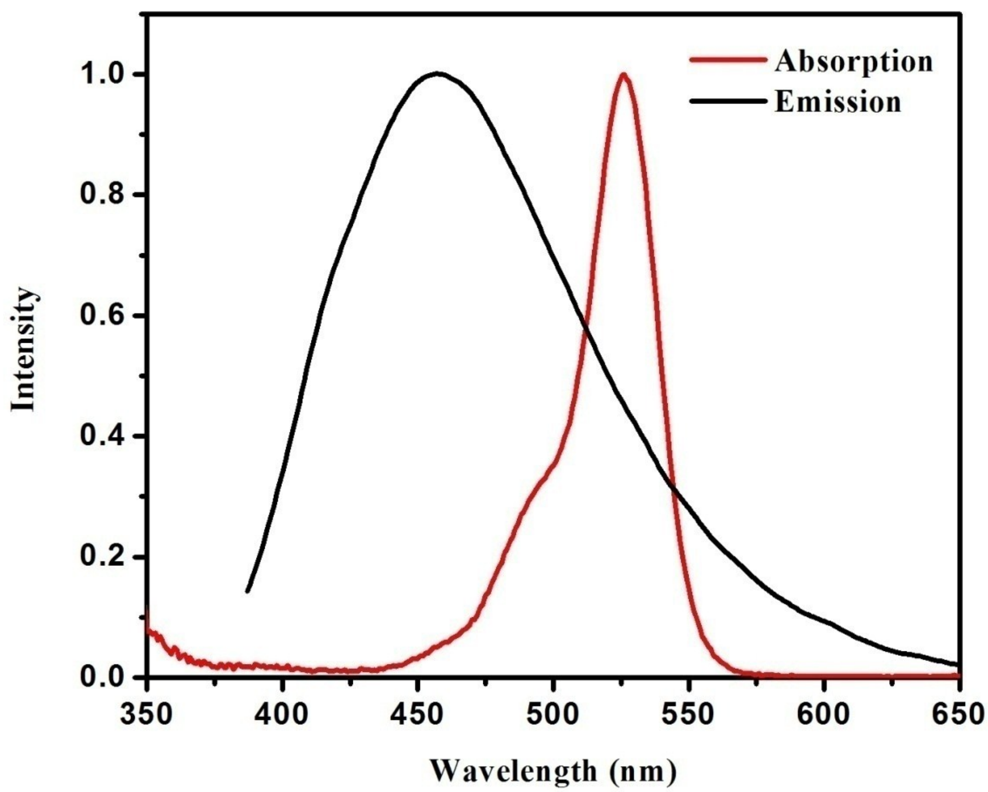

Fig. S5 Normalized absorption and emission spectrum of R6G and BMIM-NTf_2 respectively.

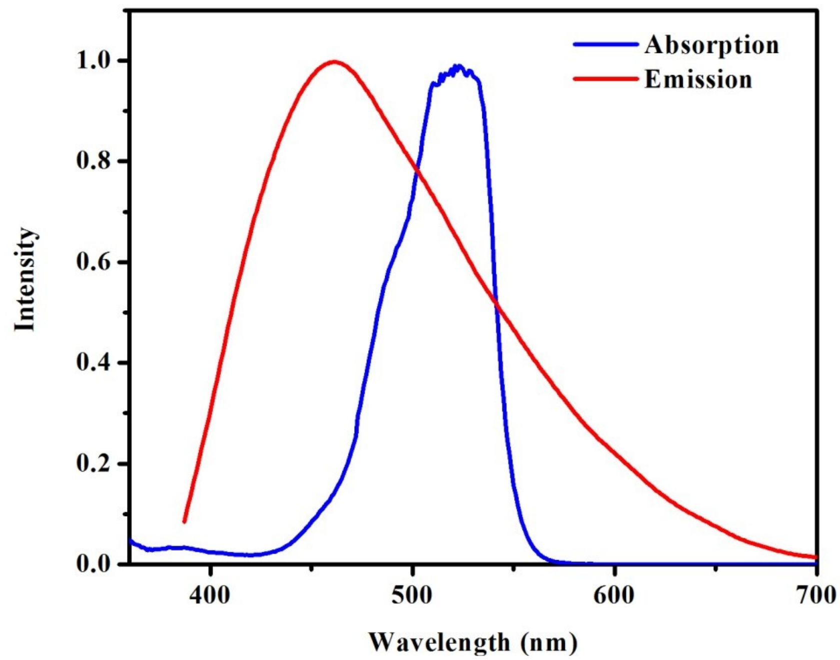

Fig. S6 Normalized absorption and emission spectrum of R6G and BMPyr-NTf2 respectively.

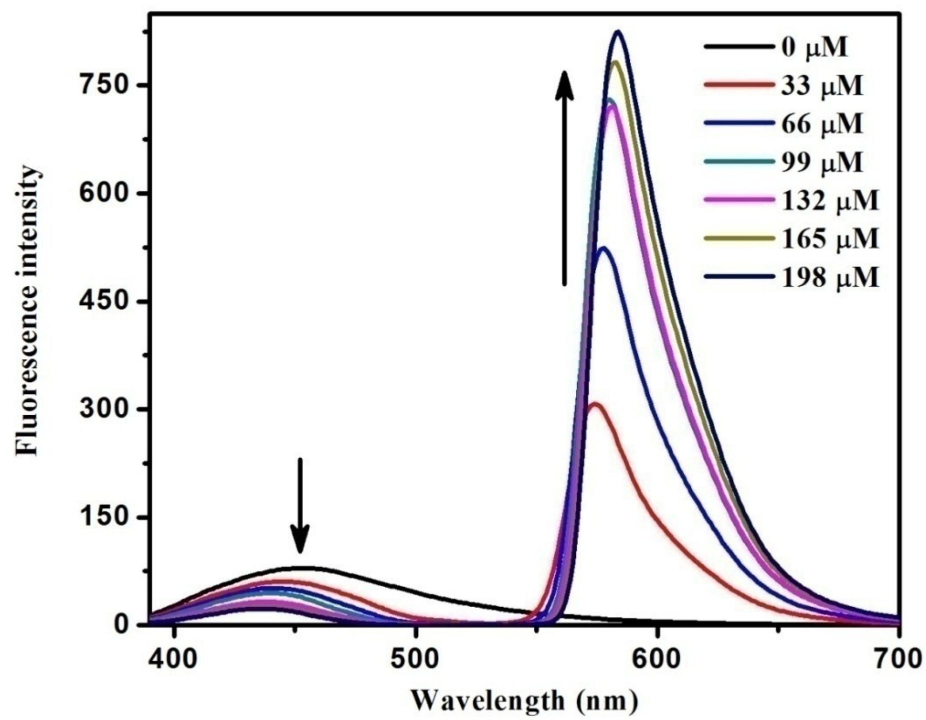

Fig. S7 Variation of emission intensity of EMIM-OS (λ_{ex}= 375 nm) upon gradual increase in the concentration of R6G.

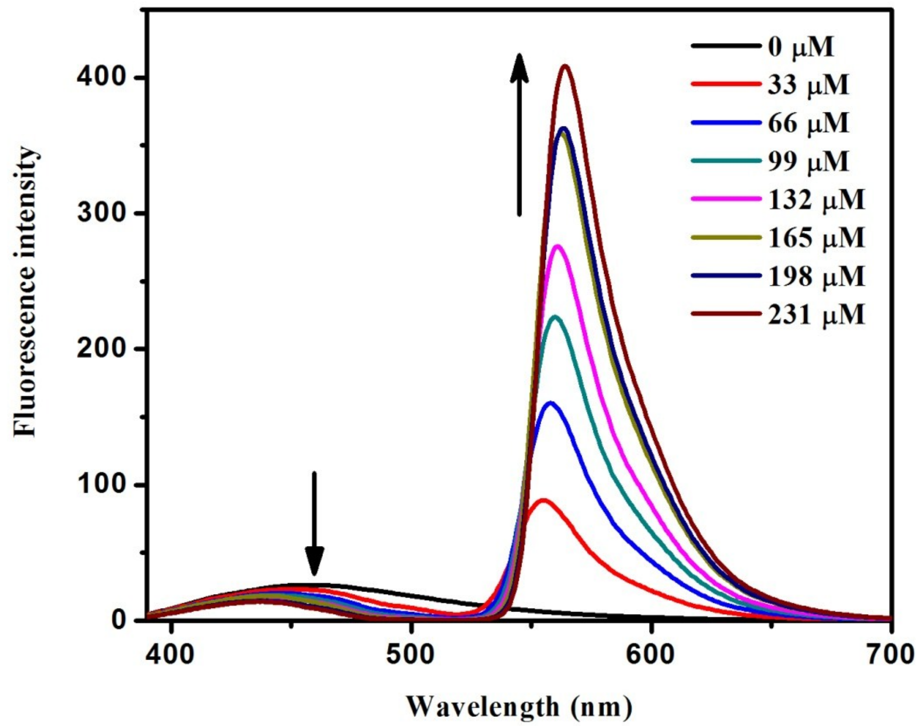

Fig. S8 Variation of emission intensity of BMIM-NTf$_2$ (λ_{ex}= 375 nm) upon gradual increase in the concentration of R6G.

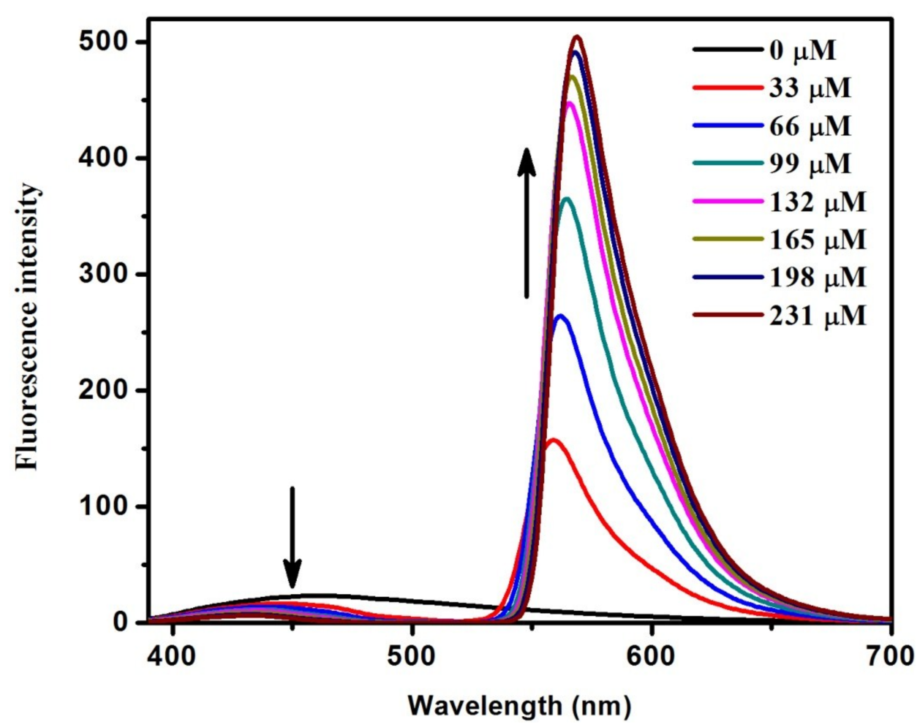

Fig. S9 Variation of emission intensity of BMPyr-NTf$_2$ (λ_{ex}= 375 nm) upon gradual increase in the concentration of R6G.

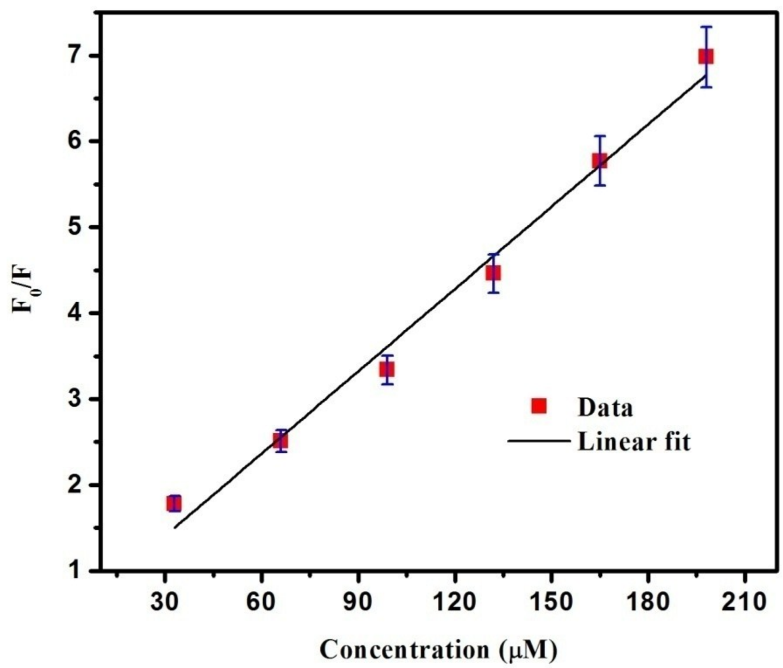

Fig. S10 Stern−Volmer plot showing a concentration variation change of fluorescence of donor (EMIM-OS). The blue lines denoted the error bar from the data points.

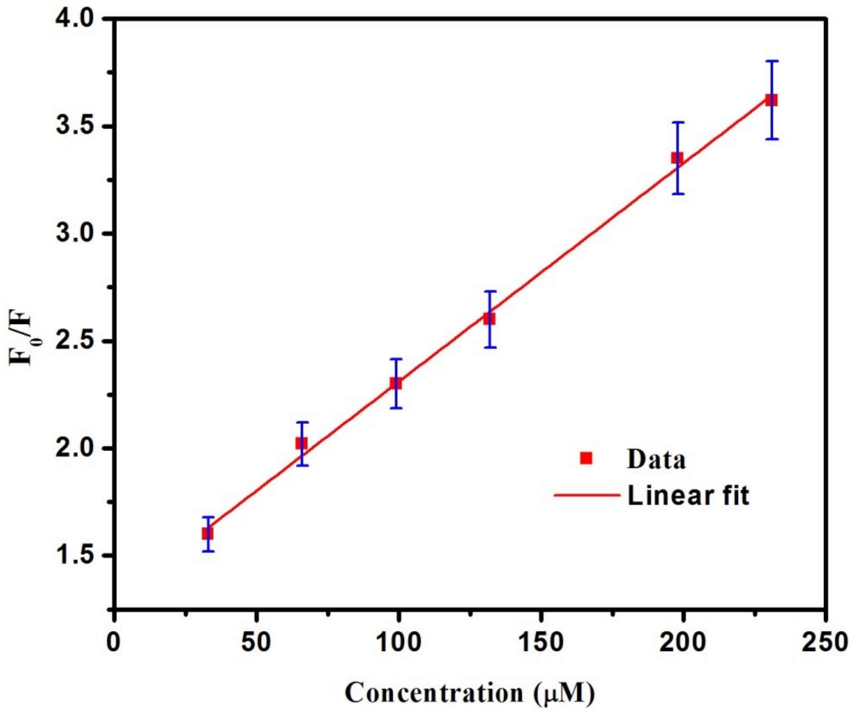

Fig. S11 Stern−Volmer plot showing a concentration variation change of fluorescence of donor (BMIM-NTf_2). The blue lines denoted the error bar from the data points.

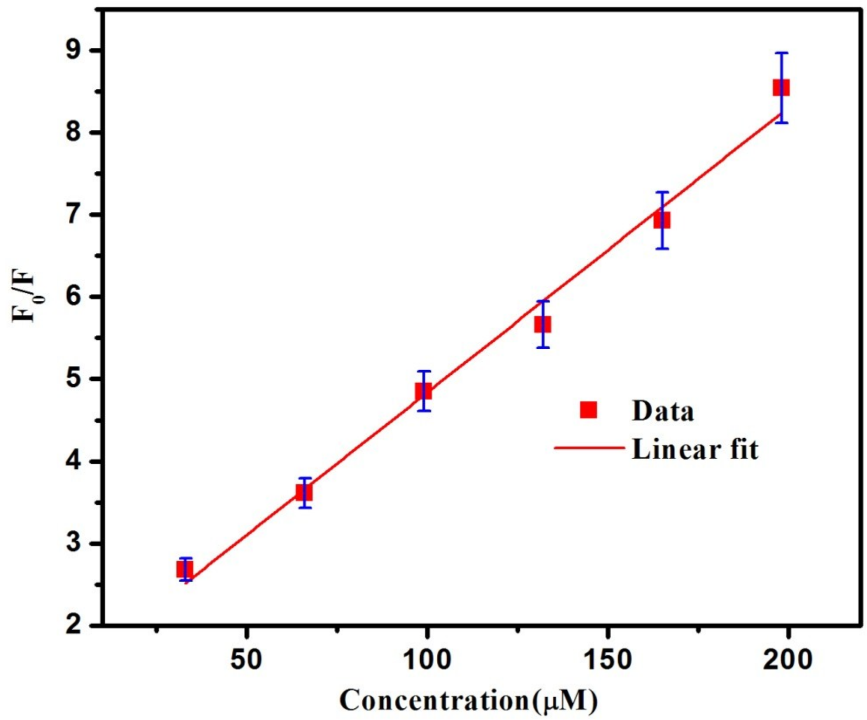

Fig. S12 Stern−Volmer plot showing a concentration variation change of fluorescence of donor (BMPyr-NTf_2). The blue lines denoted the error bar from the data points.

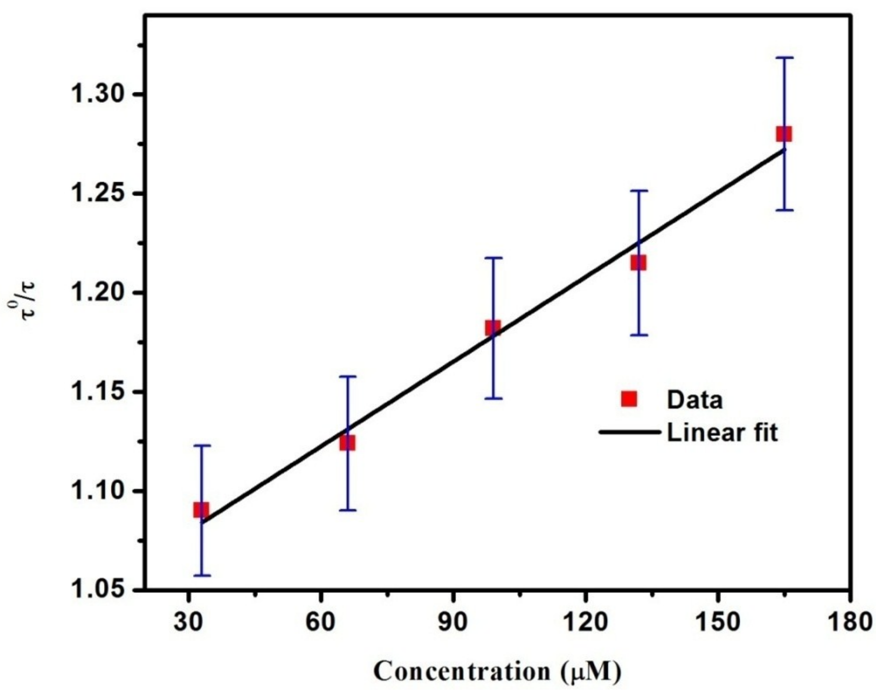

Fig. S13 Stern−Volmer plot of $\tau^0/\ \tau$ vs. concentration for EMIM-ES and R6G system. The blue lines denoted the error bar from the data points.

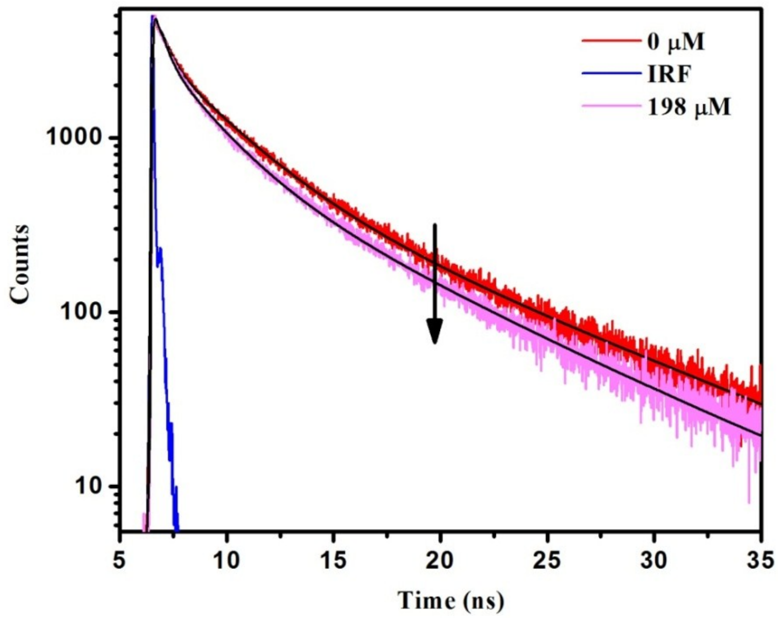

Fig. S14 Fluorescence decay curves of EMIM-OS without and in the presence of acceptor (λ_{ex}= 375 nm and λ_{em} = 450 nm). The solid black line denotes fitting to the data points. The data points are fitted by using equation 1.

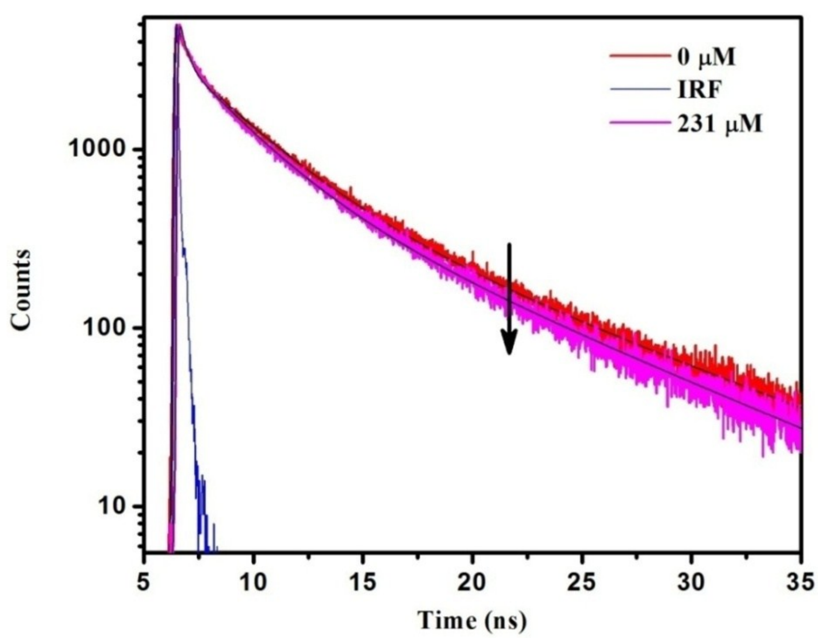

Fig. S15 Fluorescence decay curves of BMIM-NTf_2without and in the presence of acceptor (λ_{ex}= 375 nm and λ_{em} = 450 nm). The solid black line denotes fitting to the data points. The data points are fitted by using equation 1.

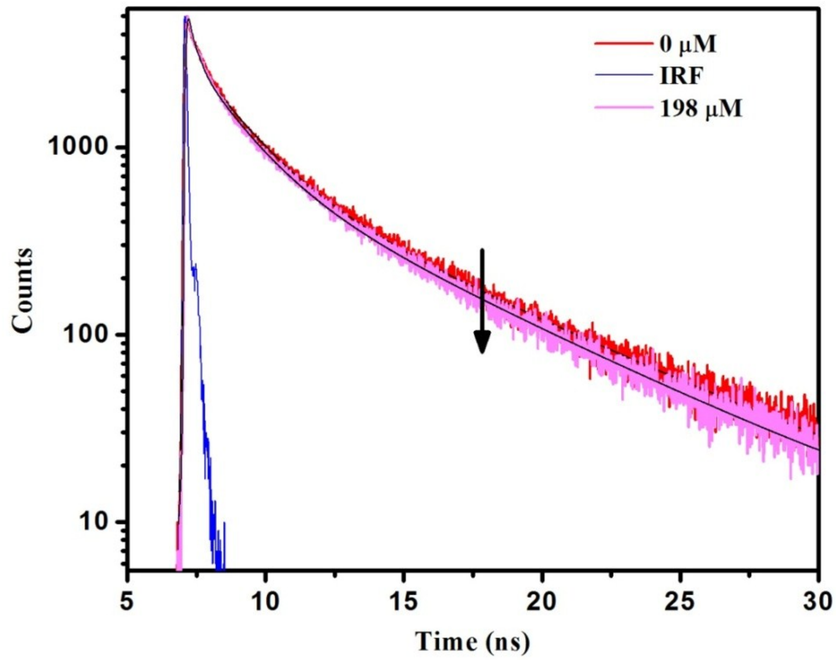

Fig. S16 Fluorescence decay curves of BMPyr-NTf_2 without and in the presence of acceptor (λ_{ex}= 375 nm and λ_{em} = 450 nm). The solid black line denotes fitting to the data points. The data points are fitted by using equation 1.

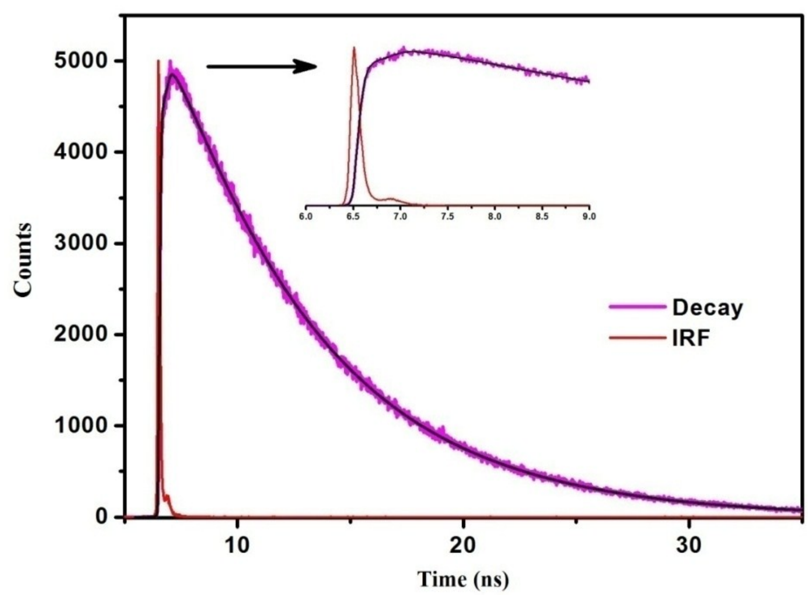

Fig. S17 Fluorescence decay curve of the acceptor (R6G) (λ_{ex} = 375 nm and λ_{em} = 573 nm; concentration of acceptor = 165 μM) in presence of EMIM-OS (IL). A clear rise has been shown in the inset. The solid black line denotes fitting to the data points. The data points are fitted by using equation 1.

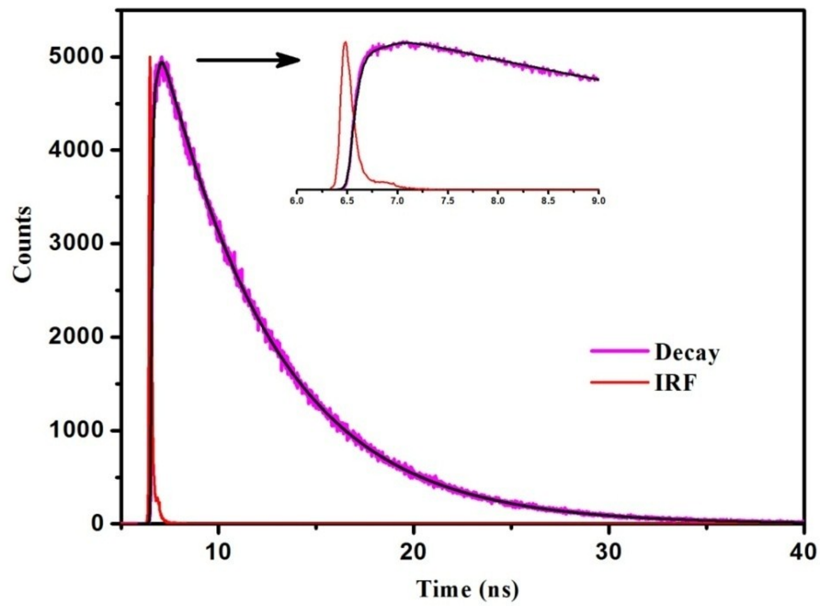

Fig. S18 Fluorescence decay curve of the acceptor (R6G) (λ_{ex} = 375 nm and λ_{em} = 566 nm; concentration of acceptor = 165 μM) in presence of BMIM-NTf_2 (IL). A clear rise has been shown in the inset. The solid black line denotes fitting to the data points. The data points are fitted by using equation 1.

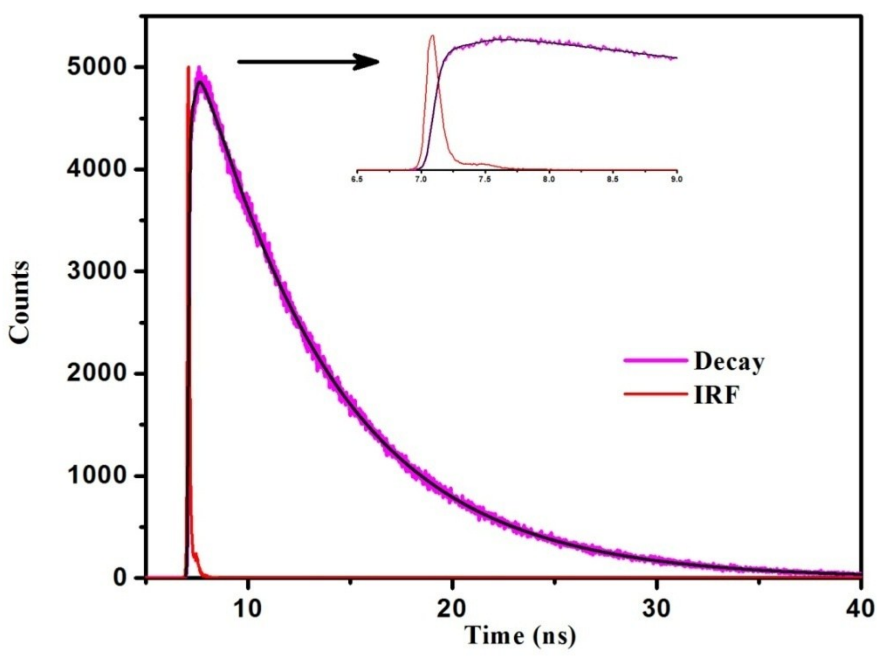

Fig. S19 Fluorescence decay curve of the acceptor (R6G) (λ_{ex} = 375 nm and λ_{em} = 556 nm; concentration of acceptor = 165 μM) in presence of BMPyr-NTf_2 (IL). A clear rise has been shown in the inset. The solid black line denotes fitting to the data points. The data points are fitted by using equation 1.

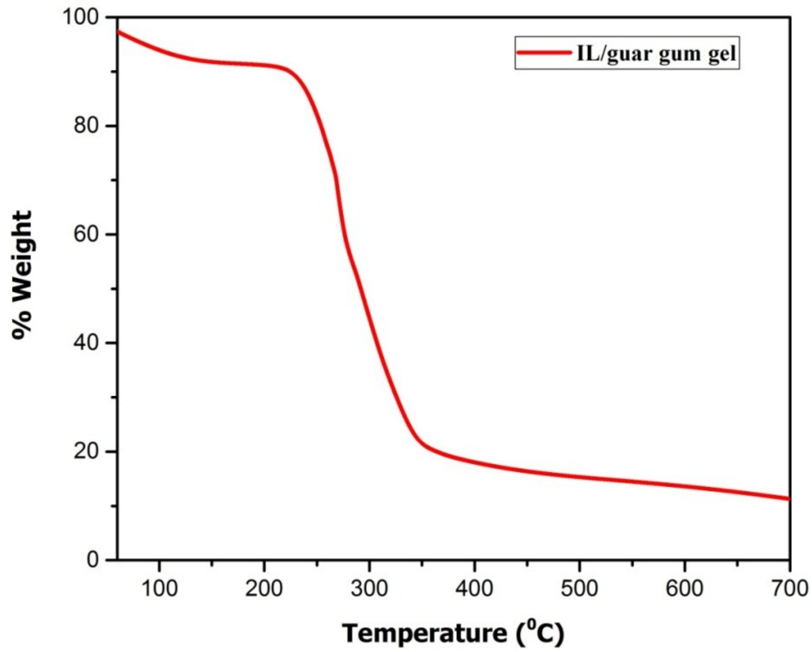

Fig. S20 Thermogravimetric analysis (TGA) spectrum of IL (EMIM-OS) /guar gum gel.

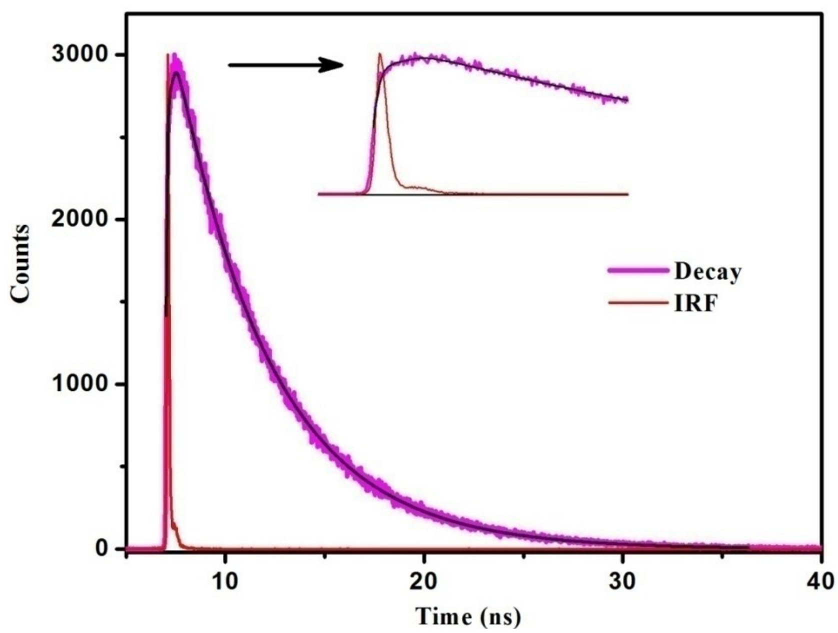

Fig. S21 Fluorescence decay curve of the acceptor (R6G) (λ_{ex} = 375 nm and λ_{em} = 580 nm) in EMIM-OS/guar gum/R6G gel system. The solid black line denotes fitting to the data points. The data points are fitted by using equation 1.

[1]H-NMR and Mass (ESI-MS) data for ionic liquids

EMIM-ES

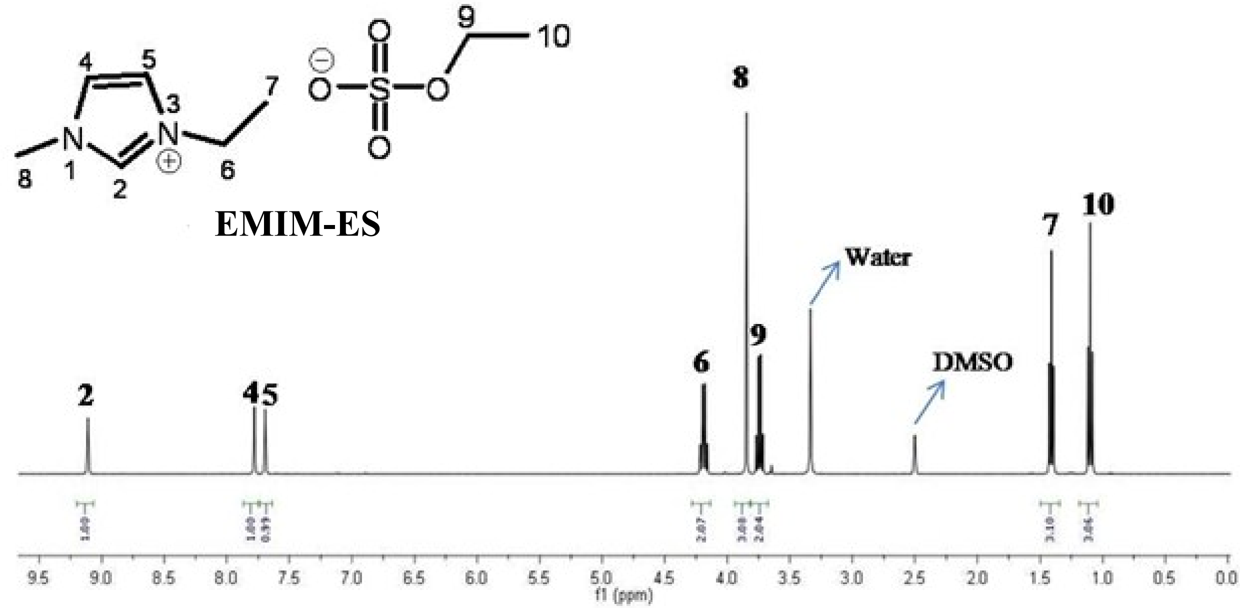

^{1}H NMR spectrum of EMIM-ES ionic liquids in DMSO-d_6

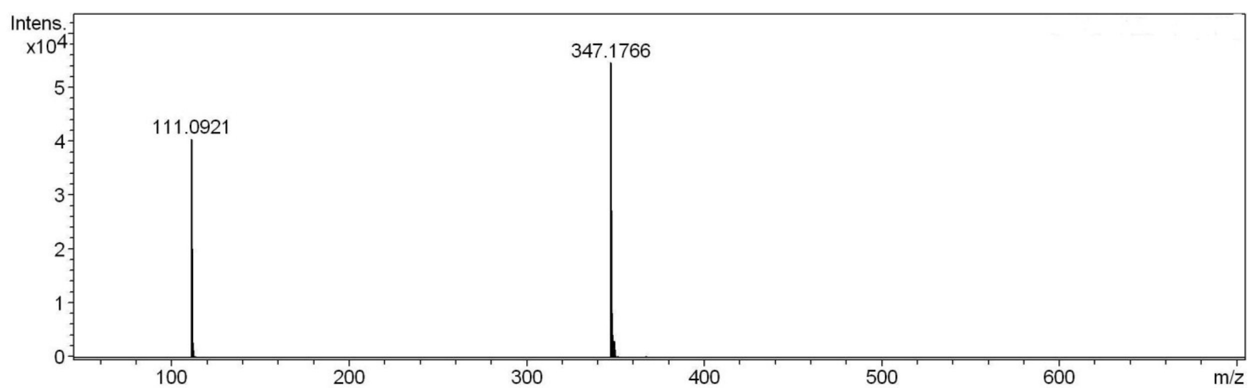

ESI-MS mass spectrum of EMIM-ES ionic liquids in methanol in the positive ion mode. The m/Z values 111.09 and 347.17 corresponds to $[EMIM]^+$ and $[(EMIM)_2(ES)]^+$ respectively. Here we note that Eberlin and coworkers have also shown the same type of fragmentation in ESI-MS mass spectrum for 1-n-butyl-3-methylimidazolium ionic liquids.[1]

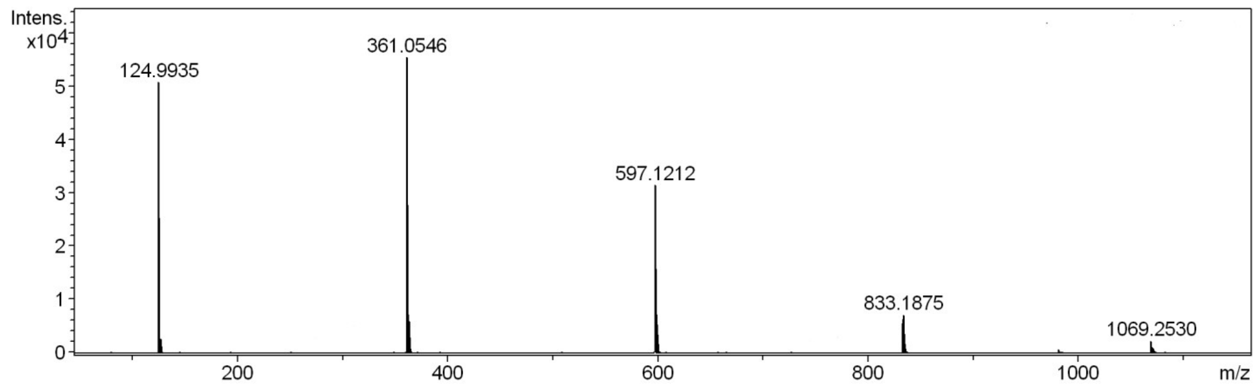

ESI-MS mass spectrum of EMIM-ES ionic liquids in methanol in the negative ion mode. The m/Z values 124.99, 361.05, 597.12, 833.187 and 1069.25 corresponds to $[ES]^-$, $[(EMIM)(ES)_2]^-$, $[(EMIM)_2(ES)_3]^-$, and $[(EMIM)_3(ES)_4]^-$ respectively.

EMIM-OS

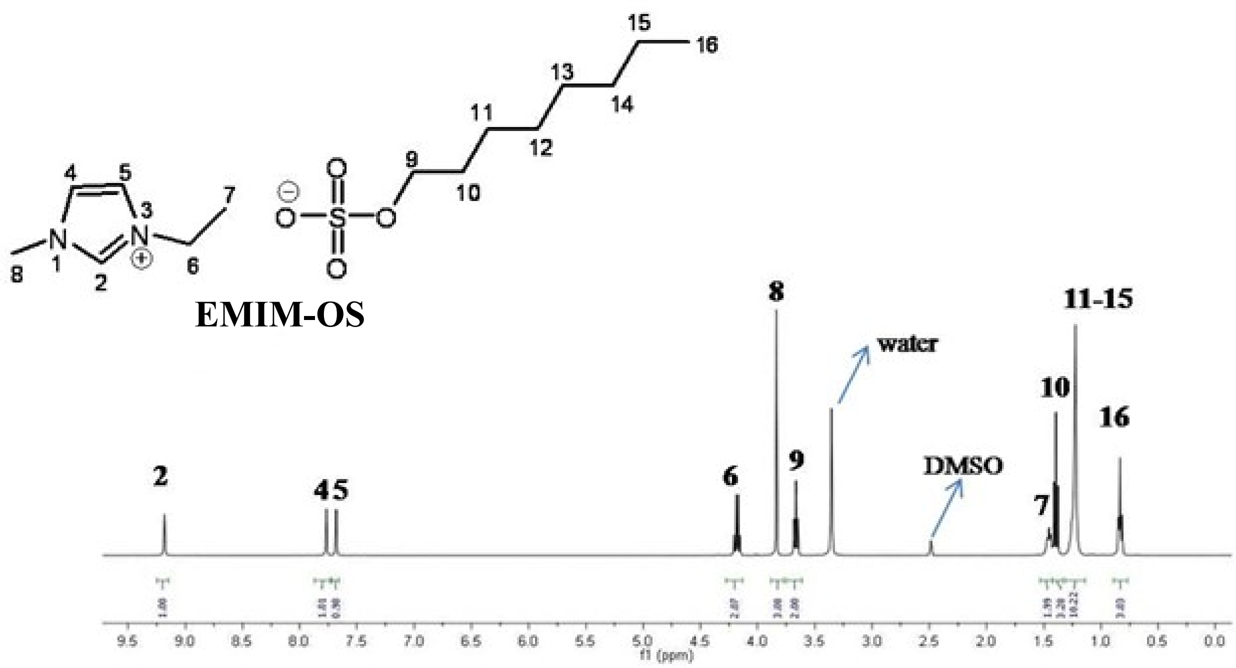

^{1}H NMR spectrum of EMIM-OS ionic liquids in DMSO-d_6

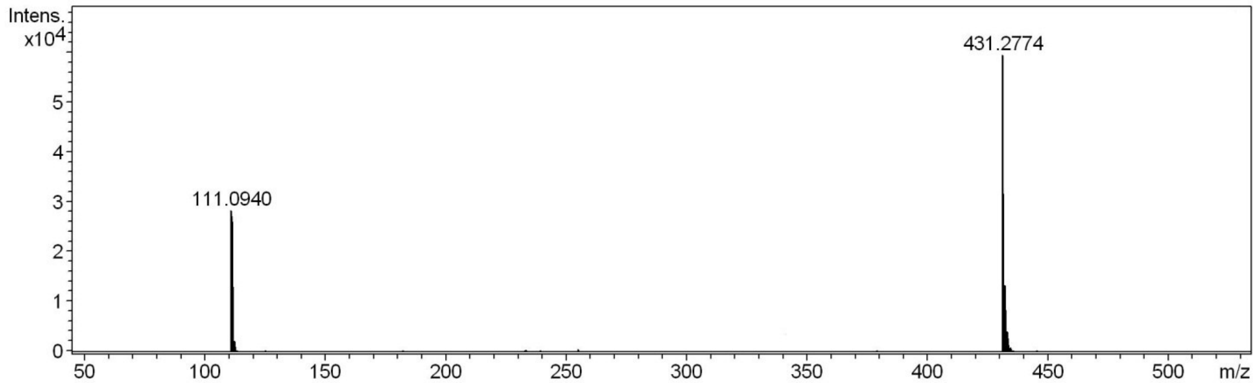

ESI-MS mass spectrum of EMIM-OS ionic liquids in methanol in the positive ion mode. The m/Z values 111.09 and 431.27 corresponds to $[EMIM]^+$ and $[(EMIM)_2OS]^+$ respectively.

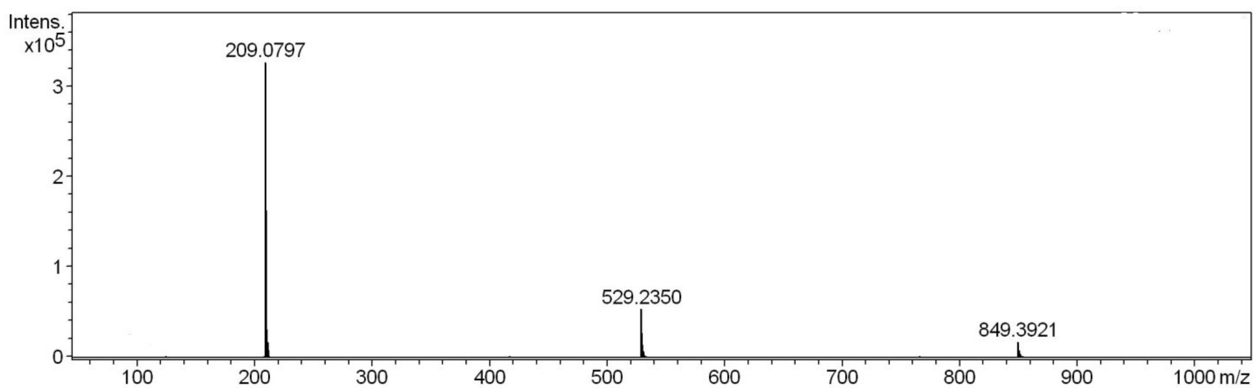

ESI-MS mass spectrum of EMIM-OS ionic liquids in methanol in the negative ion mode. The m/Z values 209.07, 529.23 and 849.39 corresponds to $[OS]^-$, $[(EMIM)(OS)_2]^-$ and $[(EMIM)_2(OS)_3]^-$ respectively.

BMIM-NTf$_2$

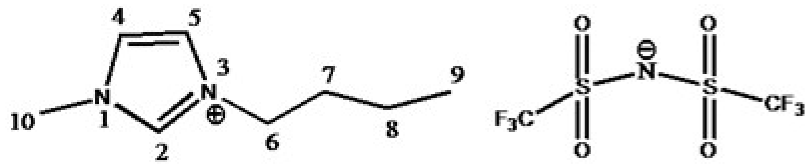

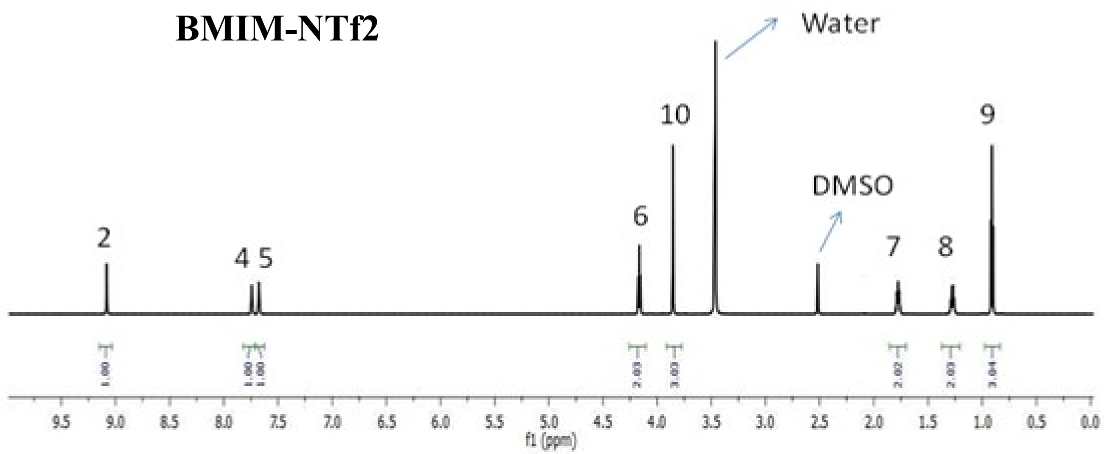

^1H NMR spectrum of BMIM-NTf$_2$ ionic liquids in DMSO-d$_6$

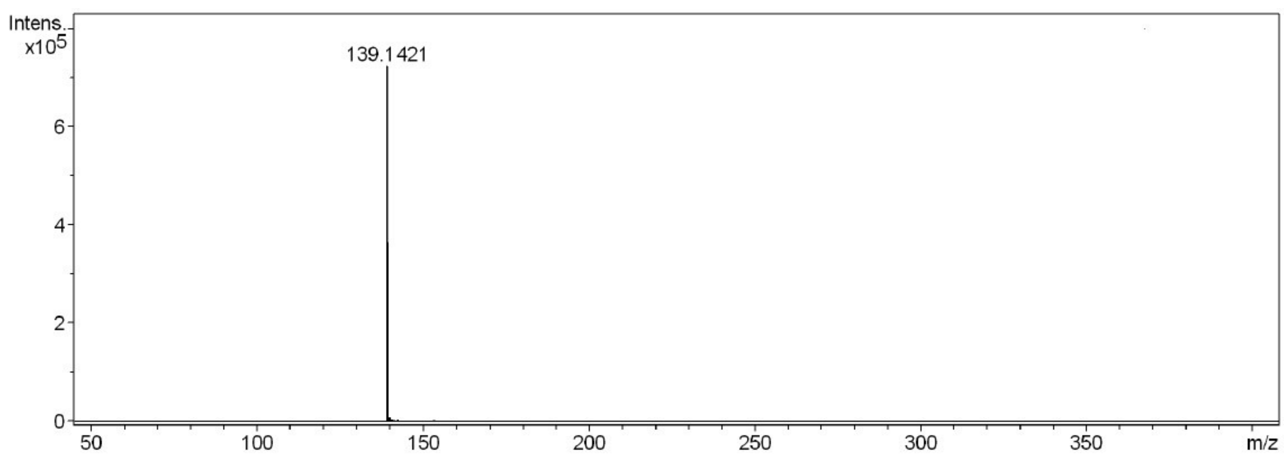

ESI-MS mass spectrum of BMIM-NTf$_2$ ionic liquids in methanol in the positive ion mode. The m/Z values 139.14 corresponds to [BMIM]$^+$.

BMPyr-NTf$_2$

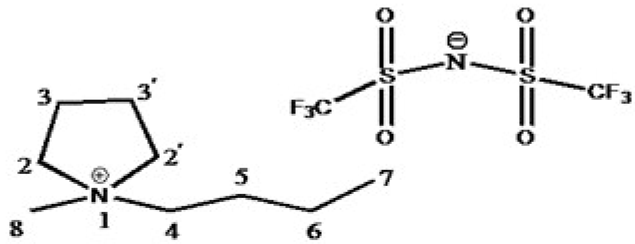

BMPyr-NTf2

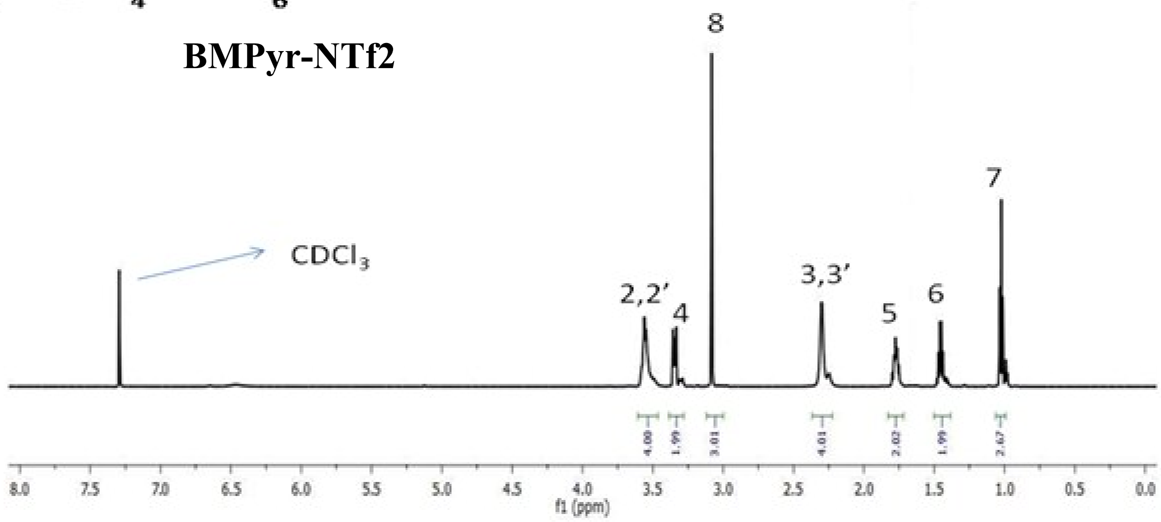

^1H NMR spectrum of BMPyr-NTf$_2$ ionic liquids in $CDCl_3$.

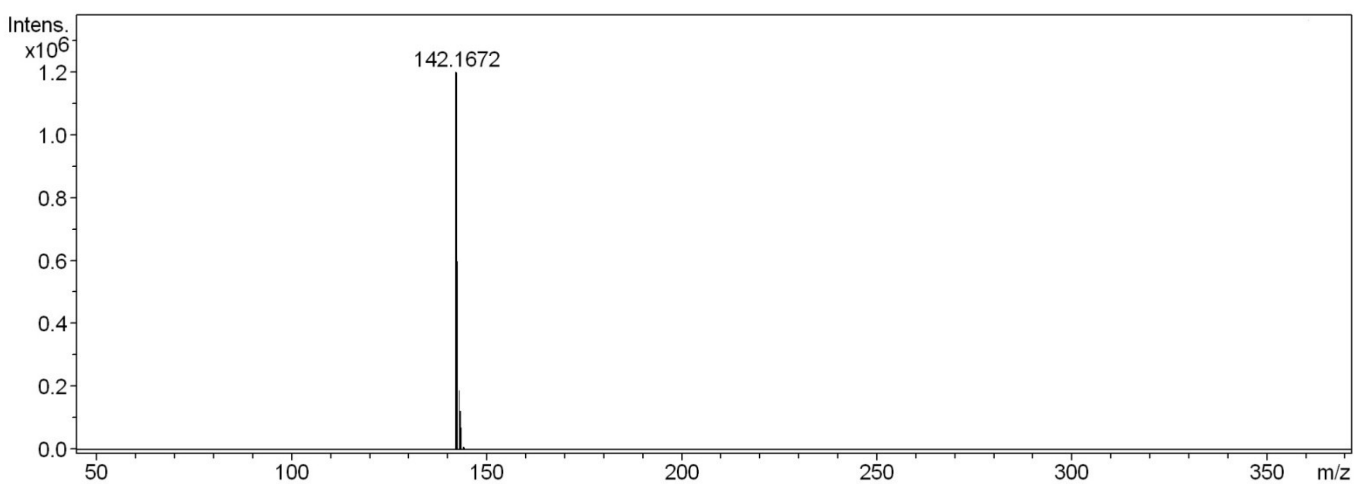

ESI-MS mass spectrum of BMPyr-NTf$_2$ ionic liquids in methanol in the positive ion mode. The m/Z values 142.146 corresponds to [BMPyr]$^+$.

Reference

(1) F. C. Gozzo, L. S. Santos, R. Augusti, C. S. Consorti, J. Dupont, and M. N. Eberlin, *Chem. Eur. J.* **2004,** *10,* 6187 – 6193.